Changsoo Jang[1]
e-mail: csjang@gmail.com

Seungbae Park

Mechanical Engineering,
State University of New York at Binghamton,
Binghamton, NY 13902-6000

Bongtae Han
Fellow, ASME

Samson Yoon

Mechanical Engineering,
University of Maryland,
College Park, MD 20742

Advanced Thermal-Moisture Analogy Scheme for Anisothermal Moisture Diffusion Problem

We propose an advanced thermal-moisture analogy scheme to cope with the inherent limitations of the existing analogy schemes. The new scheme is based on the experimentally observed unique hygroscopic behavior of polymeric materials used in microelectronics; i.e., the saturated concentration is only a function of relative humidity regardless of temperature. A new analogy formulation based on the modified solubility is presented and the scheme is implemented to investigate its accuracy and applicability. The results from a simple case study corroborate that the advanced scheme can be used effectively for package assemblies subjected to general anisothermal loading conditions.
[DOI: 10.1115/1.2837521]

1 Introduction

Moisture-related failure issues have become increasingly important as a demand for the portable electronics has increased. The analysis to determine moisture-induced deformations involves a moisture diffusion analysis and a subsequent stress analysis, where the combined effect of moisture as well as temperature distribution on the stress distribution is calculated [1].

Commercial finite element analysis (FEA) packages are ideally suited for the combined stress analysis. Most commercial FEA packages, however, do not offer the mass (or moisture) diffusion function[2] and the thermal diffusion (or heat transfer) function is utilized in practice to solve the moisture diffusion through the thermal-moisture analogies [2–4].

The thermal-moisture analogies provide an effective way to simulate the moisture diffusion but the current analogy schemes based on the uniform diffusivity or the constant solubility are valid only for (1) homogeneous material systems subjected to uniform temperature fields that could change with time or (2) multimaterial systems subjected to only isothermal loading conditions [4]. These stringent requirements limit the practice of the current analogy schemes.

In this paper, we propose an advanced thermal-moisture analogy scheme to cope with the inherent limitations of the existing schemes. The new scheme is based on the unique hygroscopic behavior of polymeric materials used in microelectronics; i.e., the saturated concentration is only a function of relative humidity regardless of temperature. The detailed analogy scheme and its implementation will be reported in the body of the text.

2 Background: Conventional Thermal-Moisture Analogies

Fick's second law describes the diffusion phenomenon inside a polymeric system as

$$\dot{C} = \nabla \cdot (D \nabla C) \tag{1}$$

where C is the moisture concentration (kg/m^3) and D is the diffusivity (m^2/s). The heat diffusion equation can be expressed as

$$\dot{q} = \rho c_p \dot{T} = \nabla \cdot (k \nabla T) \tag{2}$$

where q is the heat flux (W/m^2), T is the temperature (K), ρ is the density (kg/m^3), c_p is the specific heat (J/kg K), and k is the heat conductivity (W/mK).

Equations (1) and (2) become identical when the density and the specific heat are set to be "unity." This was referred to as "direct" analogy in Ref. [4]. The direct analogy is based on the assumption of uniform conductivity and diffusivity. Consequently, this analogy is valid only for a homogeneous material.

The maximum amount of moisture that each polymer can absorb is a material property, and thus the concentration at a bimaterial interface can be discontinuous. At a given temperature, the concentration at the interface is governed by the Nernst distribution law as [5]

$$\chi = \left. \frac{C_{\mathrm{Mat1}}}{C_{\mathrm{Mat2}}} \right|_{\mathrm{interface}} = \mathrm{const} \tag{3}$$

where χ is the Nernst partition coefficient at a specific temperature and C_{Mat1} and C_{Mat2} are the concentrations of two materials at the interface. The discontinuity can be handled mathematically by introducing the normalized concentration, which is defined as

$$\phi = \frac{C}{S} \tag{4}$$

where ϕ is the normalized concentration, and S is the solubility (sec^2/m^2).

Substituting Eq. (4) into Eq. (1), Fick's equation yields

$$\dot{S}\phi + S\dot{\phi} = \nabla \cdot [D \nabla (S\phi)] \tag{5}$$

If the solubility is uniform within the diffusing medium ($\nabla S = 0$) and is independent of time ($\dot{S} = 0$), Eq. (5) can be simplified as

$$S\dot{\phi} = \nabla \cdot (DS \nabla \phi) \tag{6}$$

Equation (6) offers another analogy scheme, referred to as "normalized" analogy in Ref. [4], where S and DS can be replaced with ρc_p and k, respectively, in the heat transfer equation. The normalized concentration in this analogy is referred to as partial

[1]Corresponding author.

Contributed by the Electrical and Electronic Packaging Division of ASME for publication in the JOURNAL OF ELECTRONIC PACKAGING. Manuscript received December 25, 2006; final manuscript received August 21, 2007; published online January 31, 2008. Review conducted by Stephen McKeown. Paper presented at the InterPACK, 2007.

[2]Only ABAQUS provides the general mass diffusion analysis capabilities but a user defined subroutine has to be developed to implement the combined analysis [1].

Table 1 Summary of measurement conditions (E, EMC; S, solder resist; C1, PWB core 1; C2, PWB core 2)

	Temp.		
RH	25°C	55°C	85°C
40%	E	E	E
45%	S, C1, C2	S, C1, C2	S, C1, C2
70%	S, C1, C2	S, C1, C2	S, C1, C2
85%	E, S, C1, C2	E, S, C1, C2	E, S, C1, C2
95%	S, C1, C2	S, C1, C2	S, C1, C2

vapor pressure [2] or wetness [3,6–9]. Although applicable to multimaterial systems, the normalized analogy is valid only when the temperature distribution is uniform and time independent [4].

3 Advanced Thermal-Moisture Analogy

3.1 Theoretical Basis of Advanced Analogy. Saturated moisture concentration is defined as the maximum moisture content at a given humidity and temperature condition. When a polymer material has weak chemical interaction with water molecule, the saturated concentration C_{sat} at the boundary of the polymer can be described by Henry's law [10] as

$$C_{sat} = SP_{VP} \tag{7}$$

where P_{VP} is the ambient vapor pressure (Pa). Using the definition of relative humidity (RH, the ratio of the vapor pressure to the saturated vapor pressure P_{sat}), Eq. (7) can be rewritten as

$$C_{sat} = S \times P_{sat} \times \mathrm{RH} \tag{8}$$

The saturated vapor pressure and solubility can be expressed by the Arrhenius relationship as [10]

$$P_{sat} = P_0 \exp\left(-\frac{E_{VP}}{RT}\right) \tag{9}$$

$$S = S_0 \exp\left(\frac{E_S}{RT}\right) \tag{10}$$

where P_0 and S_0 are the constants and E_{VP} and E_S are apparent activation energies for the vapor pressure and the solubility, respectively, and R is the gas constant (8.3145 J K^{-1} mol^{-1}). The value of P_0 and E_{VP} can be determined by fitting the pressure-temperature curve of the steam table [11]; $P_0 = 6.07 \times 10^{10}$ Pa and $E_{VP} = 0.44$ eV $= 42455$ J/mol. Combining Eqs. (8) and (10), the saturated concentration can be written as

$$C_{sat} = \left[S_0 \times P_0 \exp\left(\frac{E_S - E_{VP}}{RT}\right)\right] \times \mathrm{RH} \tag{11}$$

In their original contribution, Wong and Rajoo [12] first reported that the magnitudes of E_S for the packaging materials range from 0.44 to 0.46 eV and thus $S \times P_{sat}$ is virtually independent of temperature. Saturated concentrations of several polymers used in a ball grid array package were measured to have a further insight of this important characteristic. The material sets and test conditions are summarized in Table 1.

The polymer samples were first baked at 125°C. Moisture weight gain was measured periodically by a high precision balance (PI-225D, Denver Instrument) until the measured weight of each sample remained unchanged for an extended period of time. The saturated moisture concentration (C_{sat}) was defined as the maximum weight gain at the end of measurement. It is to be noted that the dimensions of the saturated concentration and the corresponding solubility were modified to %wt and 1/Pa, respectively, for convenience during the analysis of experimental data.

The experimental results are shown in Fig. 1, where the saturated moisture concentrations at 25°C, 55°C, and 85°C are plotted as a function of RH. It confirms that there exists a linear relationship between the saturated concentration and the RH over the temperature range used in the measurements.

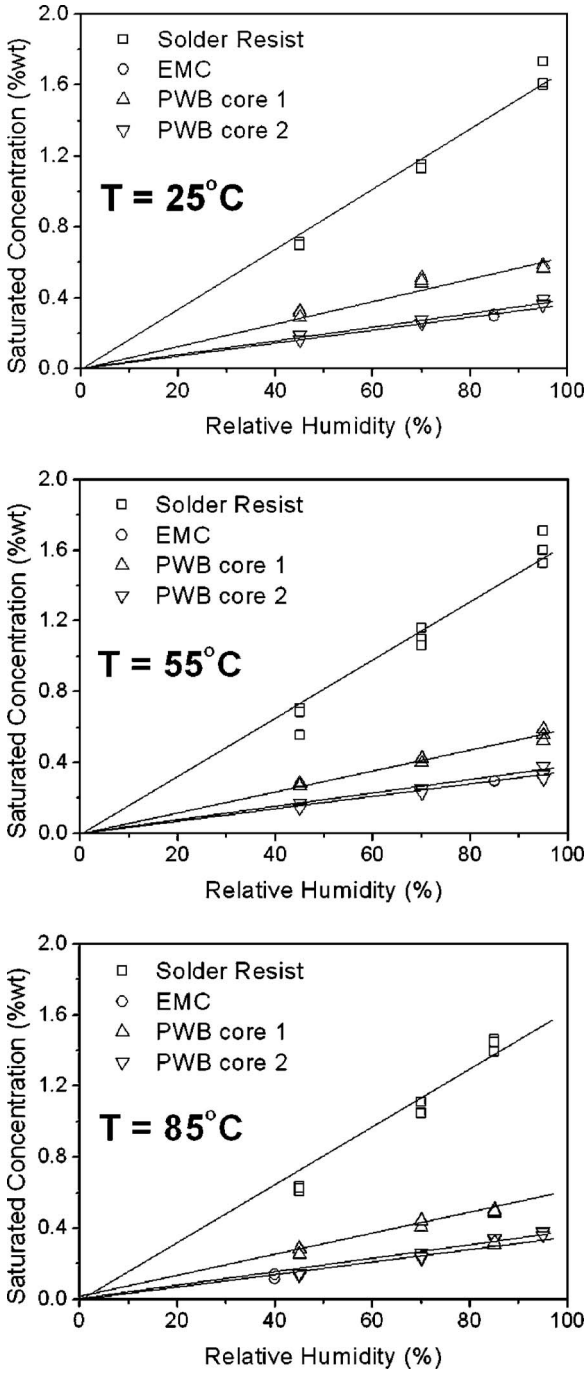

Fig. 1 Saturated concentrations as a function of RH

The values of solubility at each temperature can be determined from the saturated concentrations using Eq. (7). The solubility versus temperature is plotted in Fig. 2, where the slope represents the activation energy, E_S, of each material. The slopes are nearly identical, which indicates a constant value of activation energy.

The characteristic observed by numerous researchers [7,9,12–19] is further confirmed from Fig. 3, where the saturated concentrations at all three temperatures are plotted with respect to RH. A temperature-independent linear relation is evident for all four materials, which corroborates that $S \times P_{sat}$ is virtually inde-

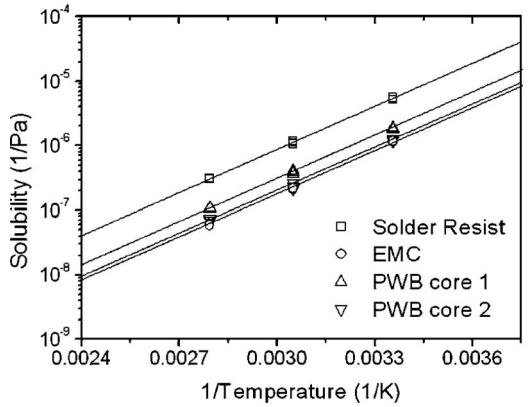

Fig. 2 Calculated solubility as a function of temperature

pendent of temperature, i.e., $E_{VP} \approx E_S$.

For these materials, C_{sat} can be represented by a linear function of RH as

$$C_{sat} \approx S_0 \times P_0 \times \mathrm{RH} = M \times \mathrm{RH} \tag{12}$$

where M is a temperature-independent property and will be referred to as "modified solubility."

3.2 Advanced Thermal-Moisture Analogy. The proposed analogy uses the modified solubility. Mathematically, a new normalized concentration φ can be defined using the modified solubility as

$$\varphi = \frac{C}{M} \tag{13}$$

It is important to note that although Eq. (13) takes a form identical to Eq. (4), the newly defined normalized concentration φ remains constant regardless of temperature. Then, using the identical approach used in the normalized analogy, the advanced thermal-moisture analogy equation can be obtained as

$$M\dot{\varphi} = \nabla \cdot (DM \nabla \varphi) \tag{14}$$

The modified solubility automatically satisfies the continuity at the interface but the boundary conditions must be modified in terms of RH. It is to be noted that the boundary conditions of the normalized analogy is the ambient vapor pressure P_{VP}.

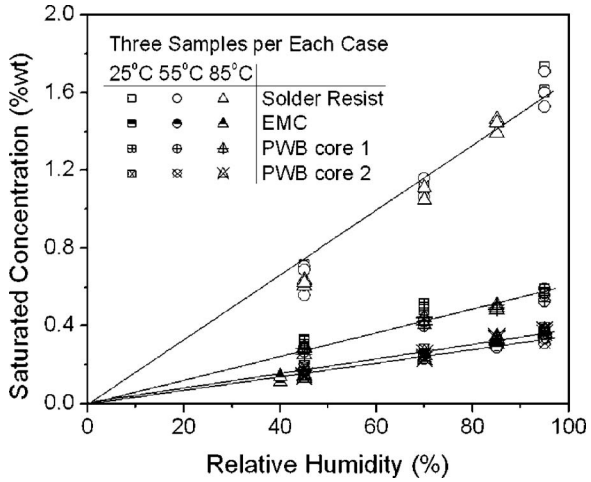

Fig. 3 Measured saturated concentration with respect to RH

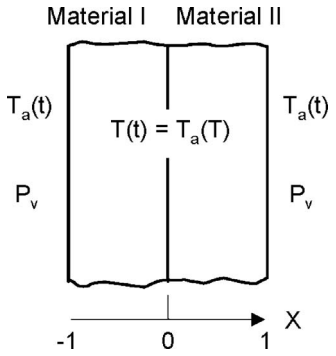

Fig. 4 Simulated geometries and boundary condition for the transient case ($\nabla T = 0$ but $\dot{T} \neq 0$)

4 Numerical Validation of Advanced Analogy

The proposed analogy was verified through two case studies. ANSYS was used to implement the proposed analogy. The mass diffusion was also solved directly by the finite difference method (FDM). The performance of the analogy scheme was verified with the numerical solution of the FDM analysis.

The specimen geometry used in the first case (referred to as "transient case") is illustrated in Fig. 4. In the transient case, the temperature has a *uniform* distribution spatially but changes with time (i.e., $\nabla T = 0$ but $\dot{T} \neq 0$) as

$$T(t) = \left(25 + \frac{1}{60}t\right)^\circ \mathrm{C} \tag{15}$$

As a result, solubility is uniform at an instant but changes with time (i.e., $\nabla S = 0$ but $\dot{S} \neq 0$).

The material properties used in the analysis are listed in Table 2. It should be noted that the activation energy of two materials is identical, which is a critical requirement for the advanced analogy. The modified solubility, M, can be calculated from Eq. (12) and they are 19.74 and 6.58 for Materials 1 and 2, respectively.

A four-node thermal element (PLANE55) was used in ANSYS for implementation of the thermal-moisture analogies. To ensure a high level of numerical accuracy, there were 200 elements through the thickness of each slab (element size of 0.0005×0.0005 mm). The initial moisture concentration in the materials is set to be "zero." The boundary condition of the new normalized concentration is defined as

$$\varphi_{BC}(t) = \frac{S(t)\phi_{BC}}{M} = \frac{S(t)P_v}{M} = \frac{S_0 P_v}{M} \exp\left[\frac{E_S}{RT(t)}\right] \tag{16}$$

The partial vapor pressure (P_v) was set at 3207 Pa (saturated vapor pressure at 25°C) and remained constant throughout the loading steps.

The case was solved using three different schemes: (1) the proposed scheme, (2) the normalized scheme (the only existing analogy scheme applicable to multimaterial cases) [4], and (3) the FDM analysis of the diffusion equations. The time step size of 2 s

Table 2 Material properties for analysis cases

	Material 1	Material 2
D_0 ($m^2\,s^{-1}$)	5×10^{-3}	4×10^{-3}
S_0 ($kg\,m^{-3}\,Pa^{-1}$)	6×10^{-10}	2×10^{-10}
E_D ($J\,mol^{-1}$)	5×10^4	5×10^4
E_S ($J\,mol^{-1}$)	4×10^4	4×10^4
c_p ($J\,kg^{-1}\,K^{-1}$)	1000	500
ρ ($kg\,m^{-3}$)	1000	1000

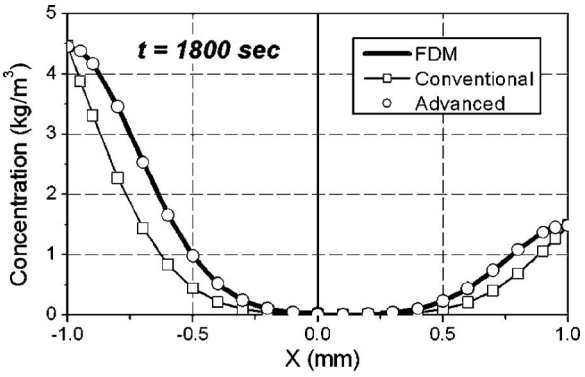

(*a*)

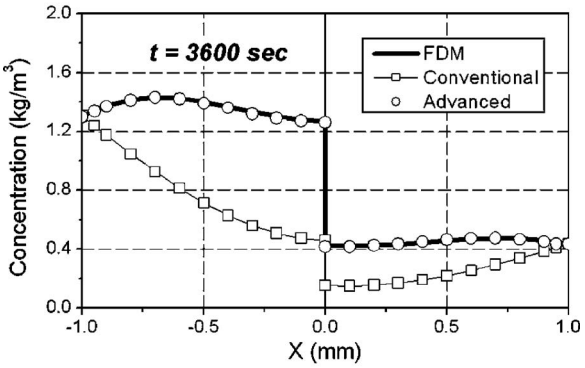

(*b*)

Fig. 5 Moisture concentrations in a bimaterial specimen subjected to the transient loading condition: (*a*) *t*=1800 s and (*b*) *t*=3600 s

was used as suggested in Ref. [4] and the details of the FDM scheme to solve the diffusion equation of the transient case can be also found in Ref. [4].

In the conventional transient heat transfer analysis, the temperature-dependent material properties at each time step are automatically updated based on the temperature calculated at the previous step. On the other hand, the independent variable in the moisture analogy is the normalized concentration. Consequently, temperature-dependent material properties should be inputted differently for implementation of the analogy scheme. The properties must be "manually" updated according to the given or calculated temperature at each time step using a custom code. An example input code for the first case is introduced in Appendix A.1.

The results are shown in Fig. 5, where the moisture concentrations determined at (*a*) 1800 s and (*b*) 3600 s are compared. The proposed scheme predicts the moisture concentration accurately, while the results of the existing normalized scheme (marked as "conventional") deviate significantly from the theoretical values, especially when the moisture concentration of each material reaches the saturated concentration (Fig. 5(*b*)). As mentioned earlier, solubility is no longer constant under anisothermal conditions (i.e., solubility becomes a function of time or $\dot{S} \neq 0$), which violates the basic constraints of all the existing analogy schemes.

A truly anisothermal case was also studied. This case (referred to as "anisothermal case") incorporates not only temperature change with time ($\dot{T} \neq 0$ and thus $\dot{S} \neq 0$) but also spatially nonuniform temperature distribution ($\nabla T \neq 0$ and thus $\nabla S \neq 0$). The geometry and the ambient temperature used in the anisothermal case are identical to those of the transient case. In the anisothermal case, the bimaterial strip is subjected to conductive as well as convective heatings, as illustrated in Fig. 6.

In order to generate a temperature gradient inside the solids the

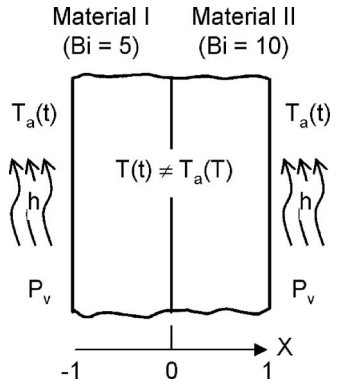

Fig. 6 Simulated geometries and boundary condition for the anisothermal case ($\nabla T \neq 0$ and $\dot{T} \neq 0$)

large Biot numbers were used in the analysis [11]; they were set 5 and 10 for Materials 1 and 2, respectively. The convection coefficient and the conductivities of two materials were set accordingly. The procedure and corresponding example input code used in the ANSYS analysis and the details of the FDM scheme to solve the anisothermal case are described in detail in Appendixes A.2 and A.3, respectively.

The temperature distributions were first determined by the FDM method at 1800 s and 3600 s and the results were compared with the results of the FEM heat transfer analysis in Fig. 7. The large temperature gradient within the bimaterial strip is evident. The corresponding results of moisture concentration are shown in Fig. 8. The proposed scheme predicts the moisture concentration accurately, which confirms that the advanced analogy is also applicable to truly anisothermal cases.

5 Conclusions

An advanced thermal-moisture analogy was proposed to cope with the limitations of the existing analogy schemes. Based on the hygroscopic characteristic of polymers used in microelectronics packing, a modified solubility was introduced, which was a temperature-invariant parameter. The proposed scheme was implemented using ANSYS and the results were validated by using numerical solutions based on the FDM. The results confirmed that the proposed scheme can be used for any anisothermal loading conditions (temporally as well as spatially) encountered in the packaging applications. The required temperature-independent linear relationship between the saturated moisture concentration

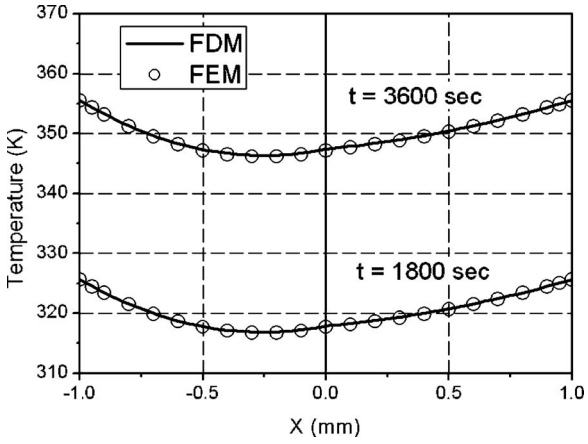

Fig. 7 Temperature distribution in a bimaterial specimen subjected to the anisothermal loading condition

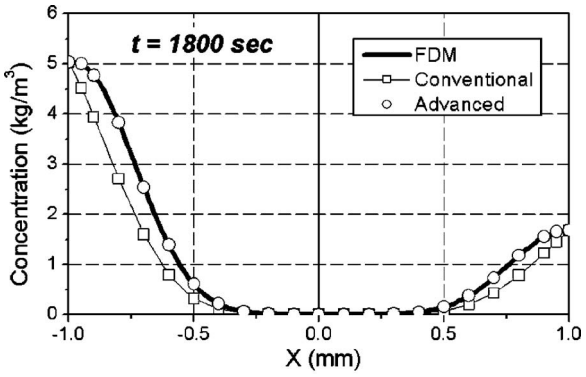

(*a*)

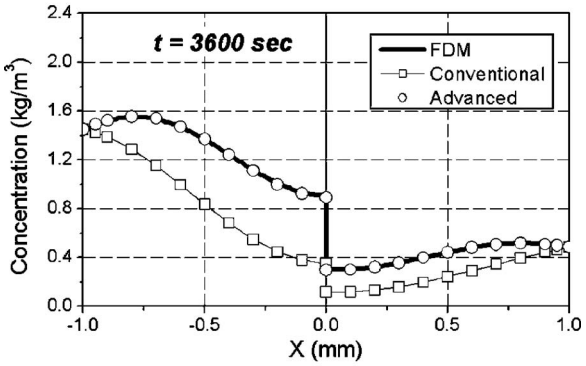

(*b*)

Fig. 8 Moisture concentrations in a bimaterial specimen subjected to the anisothermal loading condition: (*a*) *t*=1800 s and (*b*) *t*=3600 s

and the RH must be confirmed experimentally to utilize the proposed scheme accurately.

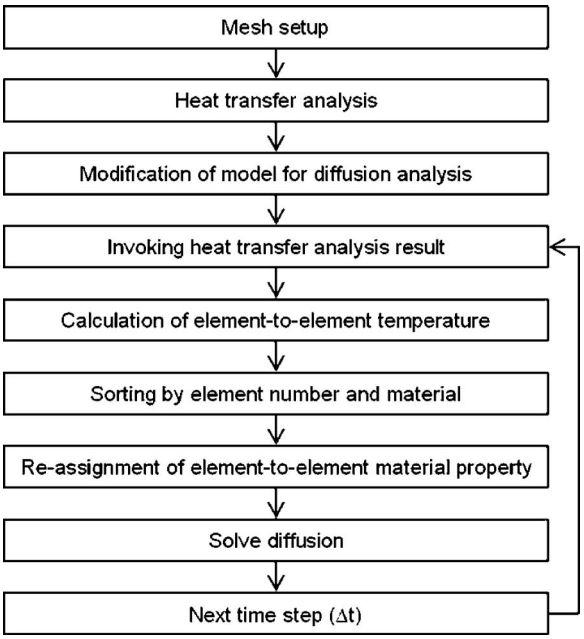

Fig. 9 General solution process of the anisothermal problem using ANSYS

Acknowledgment

This work was supported by the Integrated Electronics Engineering Center (IEEC) of the State University of New York at Binghamton and the Center for Advanced Life Cycle Engineering (CALCE) of the University of Maryland. The authors would like to thank Dr. John Lee of SUNY at Binghamton for helpful discussions on the theoretical background of the moisture diffusion equation.

Appendix: ANSYS Macros and Finite Difference Method Schemes

A.1 Transient Case ($\nabla T=0$ but $\dot{T}\neq 0$)

The macro listed below is the portion for the setup of material properties and solution steps included in the modeling program of the case study. Since the system is spatially isothermal, the properties of each material are homogenous. Therefore, they can be defined as constants at each solution step.

```
! Defining parameters
M1=19.74                    ! M of material I
M2=6.58                     ! M of material II
R_gas=8.3145                ! Gas constant
D01=5e-3                    ! D0 of material I
S01=6e-10                   ! S0 of material I
D02=4e-3                    ! D0 of material II
S02=2e-10                   ! S0 of material II
Ed1=-5e4                    ! D1=D01*exp (Ed1/R_gas/T)
Es1=4e4                     ! S1=S01*exp (Es1/R_gas/T)
Ed2=-5e4                    ! D2=D02*exp (Ed2/R_gas/T)
Es2=4e4                     ! S2=S02*exp (Es2/R_gas/T)
! RH=H0*exp (Eh/R_gas/T) for fixed partial vapor pressure (P at 25C/100%RH)
! H0=S0*Pv/M in Eq. (16), where Pv=3207 Pa in this case
H0=9.742e-8
! Note: In this program Evp was set 4e4 for consistency with Es
!       Its actual value=4.15e4
Eh=Es1                      ! Will be used to calculate phi_BC(T) for fixed Pv
T0=298                      ! Initial temperature
dt=9                        ! Time step
!
```

```
/prep7
et,1,55                                          ! 2D thermal element
c,1,M1                                           ! c=M ("Modified" solubility)
c,2,M2
dens,1,1                                         ! Densities=1
dens,2,1
!……..
! Solid modeling, meshing, and grouping for IC/BC setup
!……..
/sol
antype,4
! Initial condition setup. Node components pre-defined
! Phi of exterior surface nodes→RH of environment
ic,exterior,temp,H0*exp (Eh/T0)
! Phi of interior nodes→zero (initially fully dried)
ic,interior,temp,0
!
*do,ii,1,400
  time,ii*dt
! System temperature at the current solution step
  T1=T0+(1/60)*ii*dt
! Calculation of boundary RH at the current solution step
  d,exterior,temp,H0*exp (Eh/R_gas/T1)
! Update of conductivity of the analogy
  kxx,1,D01*exp (Ed1/R_gas/T1) *M1    ! k=DM
  kxx,2,D02*exp (Ed2/R_gas/T1) *M2
  nsub,1,1,1
  solv
*enddo
```

A.2 Anisothermal Case ($\nabla T \neq 0$ and $\dot{T} \neq 0$)

A truly anisothermal loading gives rise to much more complexity in the analogy model. An example of modeling and solving process is illustrated in Fig. 9. The key feature is re-assignment of material properties to each element after sorting all elements by materials and temperatures. In ANSYS, the element table feature [20] is useful when this process is to be implemented.

```
! key part for material property definition and update
! All parameters used in this macro are identical to those in A.1
/prep7
et,1,55              ! 2D thermal element
! Pre-definition of material properties as a function of temperature
! In this program, they are defined from 1C to 100C with one degree step
*do,ii,1,100
  dens,ii,1
  c,ii,M1
  kxx,ii,D01*exp(Ed1/(273+ii))*M1
*enddo
*do,ii,101,200
  dens,ii,1
  c,ii,M2
  kxx,ii,D02*exp(Ed2/(173+ii))*M2
*enddo
!……..
! Solid modeling, meshing, and grouping for IC/BC setup
!……..
! Total element count=8000 (4000 for each material)
! Node numbers must be controlled material-by-material (using NUMCMP)
n_total=8000
*dim,t_out,array,n_total
/sol
antype,4
!
*do,ii,1,400
  /post1
! Reading temperature distribution data from aniso_ht.rth (result file)
  file,aniso_ht,rth
  set,ii
  etable,t_res,temp          ! Element table of temperature distribution
```

```
! Storing temperature data into array
  *do,jj,1,n_total
    *get,tt1,etab,1,elem,jj
    t_out (jj)=tt1
  *enddo
  *if,ii,gt,1,then
    file,rth
  *endif
!
! Re-defining element-to-element material numbers
  /prep7
  *do,jj,1,n_total/2
    emodif,jj,mat,nint(t_out(jj)) −273
    emodif,jj+4000,mat,nint (t_out(jj+4000))−173
  *enddo
  /sol
  *if,ii,eq,1,then
    antype,trans
    ! Initial condition setup. Node components pre-defined
    ! Phi of exterior surface nodes→RH of environment
    ic,exterior,temp,H0*exp (Eh/T0)
    ! Phi of interior nodes→zero (initially fully dried)
    ic,interior,temp,0
  *else
    antype,rest
  *endif
! Environment temperature was assumed to be controlled as in A.1
! Note: Temperature inside polymers was input from the heat transfer
  T1=T0+(1/60)*ii*dt
  time,ii*dt
! Instead of ambient temperature, actual surface temperature
! has to used to calculate BC because of temperature difference
! between environment and solid surface (n_bc: node number at surface)
! If temperature is not uniform over boundary surfaces,
! BC should be input node-to-node
  d,exterior,temp,t_out(n_bc)
  nsub,1,1,1
  solv
*enddo
```

From a practical point of view, the spatially anisothermal complexity is not needed for most of problems since spatial temperature gradients during heating or cooling can be ignored (usually less than 1 °C). In addition, the time step can be controlled in an automatic manner by implementing a customized macro for time step adjustment while taking the rate of concentration change at each step into consideration.

A.3 Finite Difference Method Schemes for Anisothermal Case ($\nabla T \neq 0$ and $\dot{T} \neq 0$)

Reference [4] describes in detail a FDM scheme for a transient diffusion analysis. Since the second case considered in this paper considers a spatially anisothermal temperature distribution, the gradient of the diffusivity and solubility has to be incorporated in the FDM scheme.

The finite difference form of the divergence term in the diffusion equation can be expressed as

$$\frac{d}{dx}\left(D_x^t \frac{dC_x^t}{dx}\right) = \frac{d}{dx}\left[D_x^t \frac{d(S_x^t \phi_x^t)}{dx}\right] = \frac{\left(\frac{D_{x+\Delta x}^t + D_x^t}{2}\right)\frac{S_{x+\Delta x}^t \phi_{x+\Delta x}^t - S_x^t \phi_x^t}{\Delta x} - \left(\frac{D_x^t + D_{x-\Delta x}^t}{2}\right)\frac{S_x^t \phi_x^t - S_{x-\Delta x}^t \phi_{x-\Delta x}^t}{\Delta x}}{\Delta x}$$

$$= \frac{(D_x^t + D_{x-\Delta x}^t)S_{x-\Delta x}^t \phi_{x-\Delta x}^t - (D_{x+\Delta x}^t + 2D_x^t + D_{x-\Delta x}^t)S_x^t \phi_x^t + (D_{x+\Delta x}^t + D_x^t)S_{x+\Delta x}^t \phi_{x+\Delta x}^t}{2(\Delta x)^2}$$

The proposed analogy scheme is mathematically equivalent to the original diffusion equation as far as the exponents of solubility equations are identical. One can take the finite difference form of the advanced analogy scheme to solve the diffusion, which is simpler, faster, and possibly more accurate by eliminating the exponentially changing solubility terms. It can be expressed mathematically as

$$\frac{d}{dx}\left(D_x^t \frac{dC_x^t}{dx}\right) = \frac{d}{dx}\left[D_x^t \frac{d(M\varphi_x^t)}{dx}\right] = \frac{d}{dx}\left(MD_x^t \frac{d\varphi_x^t}{dx}\right) = M\frac{\left(\frac{D_{x+\Delta x}^t + D_x^t}{2}\right)\frac{\varphi_{x+\Delta x}^t - \varphi_x^t}{\Delta x} - \left(\frac{D_x^t + D_{x-\Delta x}^t}{2}\right)\frac{\varphi_x^t - \varphi_{x-\Delta x}^t}{\Delta x}}{\Delta x}$$

$$= M\frac{(D_x^t + D_{x-\Delta x}^t)\varphi_{x-\Delta x}^t - (D_{x+\Delta x}^t + 2D_x^t + D_{x-\Delta x}^t)\varphi_x^t + (D_{x+\Delta x}^t + D_x^t)\varphi_{x+\Delta x}^t}{2(\Delta x)^2}$$

References

[1] Yoon, S., Han, B., Cho, S., and Jang, C., 2005, "Non-Linear Finite Element Analysis for Electronic Packages Subjected to Combined Hygroscopic and Thermo-Mechanical Stresses," *Proceedings of Pacific Rim/ASME International Electronic Packaging Technical Conference and Exhibition*, IPACK Paper No. 2005-73427.

[2] Galloway, J. E., and Miles, B. M., 1997, "Moisture Absorption and Desorption Predictions for Plastic Ball Grid Array Packages," IEEE Trans. Compon., Packag. Manuf. Technol., Part A, **20**(3), pp. 274–279.

[3] Wong, E. H., Teo, Y. C., and Lim, T. B., 1998, "Moisture Diffusion and Vapor Pressure Modeling of IC Packaging," *Proceedings of 38th Electronic Components and Technology Conference*, Seattle, pp. 1372–1378.

[4] Yoon, S., Han, B., and Wang, Z., 2007, "On Moisture Diffusion Modeling Using Thermal Diffusion Analogy," J. Electron. Packag., **129**, pp. 421–426.

[5] Jost, W., 1960, *Diffusion in Solids, Liquids, Gases*, 3rd ed., Academic, New York.

[6] Puig, O., Martinot, C., and Roustan, P., 1998, "Moisture Ingress and Absorption in a CCD Package Characterisation, Modelisation and Measurement," *Proceedings of the POLY'98*, France, pp. 1–7.

[7] Wong, E. H., Chan, K. C., Tee, T. Y., and Rajoo, R., 1999, "Comprehensive Treatment of Moisture Induced Failure in IC Packaging," *Proceedings of the Third Electronics Manufacturing Technology Conference*, Japan, pp. 176–181.

[8] Wong, E. H., Rajoo, R., Koh, S. W., and Lim, T. B., 2002, "The Mechanics and Impact of Hygroscopic Swelling of Polymeric Materials in Electronic Packaging," ASME J. Electron. Packag., **124**, pp. 122–126.

[9] Wong, E. H., Koh, S. W., Lee, K. H., and Rajoo, R., 2002, "Comprehensive Treatment of Moisture Induced Failure—Recent Advances," IEEE Trans. Electron. Packag. Manuf., **25**, pp. 223–230.

[10] Osswald, T., and Menges, G., 1996, *Materials Science of Polymers for Engineers*, Hanser-Gardener, Munich.

[11] Incropera, F. P., and DeWitt, D. P., 2002, *Fundamentals of Heat and Mass Transfer*, 5th ed., Wiley, New York.

[12] Wong, E. H., and Rajoo, R., 2003, "Moisture Absorption and Diffusion Characterization of Packaging Materials—Advanced Treatment," Microelectron. Reliab., **43**, pp. 2087–2096.

[13] Tay, A. A. O., and Lin, T. Y., 1998, "Moisture-Induced Interfacial Delamination Growth in Plastic IC Packages During Solder Reflow," *Proceedings of 38th Electronic Components and Technology Conference*, Seattle, pp. 371–378.

[14] Uschitsky, M., and Suhir, E., 2001, "Moisture Diffusion in Epoxy Molding Compounds Filled With Particles," ASME J. Electron. Packag., **123**, pp. 47–51.

[15] Chang, K. C., Yeh, M. K., and Chiang, K. N., 2004, "Hygrothermal Stress Analysis of a Plastic Ball Grid Array Package During Solder Reflow," Proc. Inst. Mech. Eng., Part C: J. Mech. Eng. Sci., **218**, pp. 957–970.

[16] Chen, X., Zhao, S., and Zhai, L., 2005, "Moisture Absorption and Diffusion Characterization of Molding Compound," ASME J. Electron. Packag., **127**, pp. 460–465.

[17] Yoon, S., Han, B., Cho, S., and Jang, C., 2005, "Experimental Verification of Non-Linear Finite Element Analysis for Combined Hygroscopic and Thermo-Mechanical Stresses," *Proceedings of 2005 SEM Annual Conference*, Portland.

[18] Vogels, R. C. J., Huang, M., Yang, D. G., van Driel, W. D., and Zhang, G. Q., 2005, "Fast Characterization for Moisture Properties of Moulding Compounds: Influence of Temperature and Humidity," *Proceedings of the Sixth International Conference on Electronic Packaging Technology*, China, pp. 185–190.

[19] Jang, C., Han, S., Kim, Y., Kim, H., Yoon, S., Cho, S., Han, C., and Han, B., 2005, "Development of Predictive Modeling Scheme for Flip-Chip on Fine Pitch Flex Substrate," *Proceedings of EuroSimE 2005*, Berlin.

[20] 2005, ANSYS Release 9 Documentation.